Article

Not peer-reviewed version

Preparation and Electrocatalytic Activity of Bimetallic Ni-Cu Micro- and Nanoparticles

Nina M. Ivanova *, Zainulla M. Muldakhmetov, Yelena A. Soboleva, Yakha A. Vissurkhanova, Moldir E. Beisenbekova

Posted Date: 7 July 2023

doi: 10.20944/preprints202307.0455.v1

Keywords: Bimetallic micro- and nanoparticles; chemical successive reduction; electrocatalysts; electrocatalytic hydrogenation; p-aminophenol

Article

Preparation and Electrocatalytic Activity of Bimetallic Ni-Cu Micro- and Nanoparticles

Nina M. Ivanova *, Zainulla M. Muldakhmetov, Yelena A. Soboleva, Yakha A. Vissurkhanova and Moldir E. Beisenbekova

Institute of Organic Synthesis and Chemistry of Coal of Kazakhstan Republic, Alikhanov Str., 1, Karaganda 100000, Kazakhstan; iosu.rk@mail.ru (Z.M.M); esoboleva-kz@mail.ru (Y.A.S.); yakhavisurkhanova@bk.ru (Y.A.V.); monika_99@list.ru.

* Correspondence: nmiva@mail.ru (N.I.)

Abstract: Bimetallic Ni/Cu core-shell and Cu-Ni heterostructural micro- and nanoparticles were prepared using two simple successive reduction procedures. Monometallic Ni and Cu particles were synthesized for comparison. The phase constitutions and morphological features of the particles were studied by means of X-ray diffraction, energy-dispersive X-ray spectroscopy and scanning electron microscopy methods. All the obtained mono- and bimetallic particles were applied as electrocatalysts in the electrohydrogenation of *p*-nitrophenol (*p*-NPh). An additional electrochemical reduction of copper cationsduring the hydrogen saturation of Cu-containing particles was established. Some of the prepared particles exhibited high catalytic activity with an increase in the hydrogenation rate of *p*-NPh by more than 3 times compared to its electrochemical reduction on the non-activated cathode, and *p*-NPh conversion yielded the maximum values. The main product of *p*-NPh electrocatalytic hydrogenation over Ni-Cu particles is *p*-aminophenol, which is an intermediate in the synthesis of many drugs. *p*-Aminophenol formation is confirmed by UV-Vis spectra.

Keywords: bimetallic micro- and nanoparticles; chemical successive reduction; electrocatalysts; electrocatalytic hydrogenation; *p*-aminophenol

1. Introduction

Bimetallic nanoparticles (NPs) generally have several improved properties compared to monometallic analogs, and depending on the synthesis method and conditions, they can be created with different structures and phase compositions: alloys, core-shells, "two-faced" Janus particles, interacting aggregates, and heterostructures [1-4]. In the literature, various methods for obtaining bimetallic nanoparticles in the form of core-shell are described, such as thermal decomposition of the corresponding precursors [5], decomposition upon irradiation [6], chemical reduction [7, 8], hydrothermal method [9], and so on. In turn, chemical reduction methods are subdivided into the co-reduction of metals, the reduction of bimetallic complexes and the successive reduction.

An analysis of the literature has shown that to prepare bimetallic nanoparticles in the form of a core-shell including Ni-Cu NPs, a two-stage strategy is most often used: firstly, nanoparticles of one metal are obtained using various methods of chemical reduction of this metal cations from its precursor; then a layer of the second reduced metal is deposited on the NPs of the first metal. According to this strategy, Cu/Ni [10–13] and Ni/Cu [11, 14] core-shell nanoparticles were synthesized using various metal precursors, solvents, reducing agents, stabilizers, and, in general, different procedures. Furthermore, Cu/Ni and Ni/Cu micro- and nanoparticles were prepared by joint reduction of cations of both metals from their hydroxides in water-ethylene glycol solution [15], by electrodeposition [16], microwave radiation [6], solution combustion synthesis [17] and other methods. The resulting bimetallic Ni-Cu nanoparticles as a rule were tested for the manifestation of catalytic, photocatalytic and electrocatalytic activity as well as their magnetic properties depending on the ratio of metals. The advantages of bimetallic Ni-Cu particles with core-shell structure include, firstly, the possibility of influencing such particles with magnet due to the fact that the nickel core

Preprints (www.preprints.org) | NOT PEER-REVIEWED | Posted: 7 July 2023 doi:10.20944/preprints202307.0455.v1

has magnetic properties and secondly, the coating of nickel particles with copper shell protects the core from air oxidation.

This paper presents the results of studies of the electrocatalytic properties of bimetallic Ni-Cu particles in the process of electrocatalytic hydrogenation of p-nitrophenol (*p*-NPh). The created bimetallic Ni-Cu particles have various sizes and shapes, including core-shell and heterostructure, which are determined by the chemical reduction conditions. Powders of bimetallic Ni-Cu particles possessing magnetic properties are held on the cathode surface by an external magnet. The product of the *p*-NPh electrocatalytic hydrogenation is *p*-aminophenol (*p*-APh), which is widely used in various fields of industry and in particular in the pharmaceutical industry for the production of drugs, for example, acetaminophen and many other drugs based on it. It should be noted that there are many studies in the literature that have tested the developed catalytic systems in the transformation of nitrophenols, which are environmentally hazardous toxic substances, to aminophenols, for example, in [18–24]. Bimetallic Ni/Cu nanowires synthesized by a liquid phase reduction also exhibited attractive catalytic characteristics in this process [25].

2. Results and discussion

Monometallic Ni and Cu particles were prepared by chemical reduction in an aqueous-ethanol solution and according to XRD analysis, nickel cations were almost completely reduced. In the XRD pattern (Figure 1, a), the strong diffraction peaks correspond to the crystalline phases of nickel. There is also a small admixture of nickel (II) hydroxide, which is formed in the alkaline solution at the cations reduction.

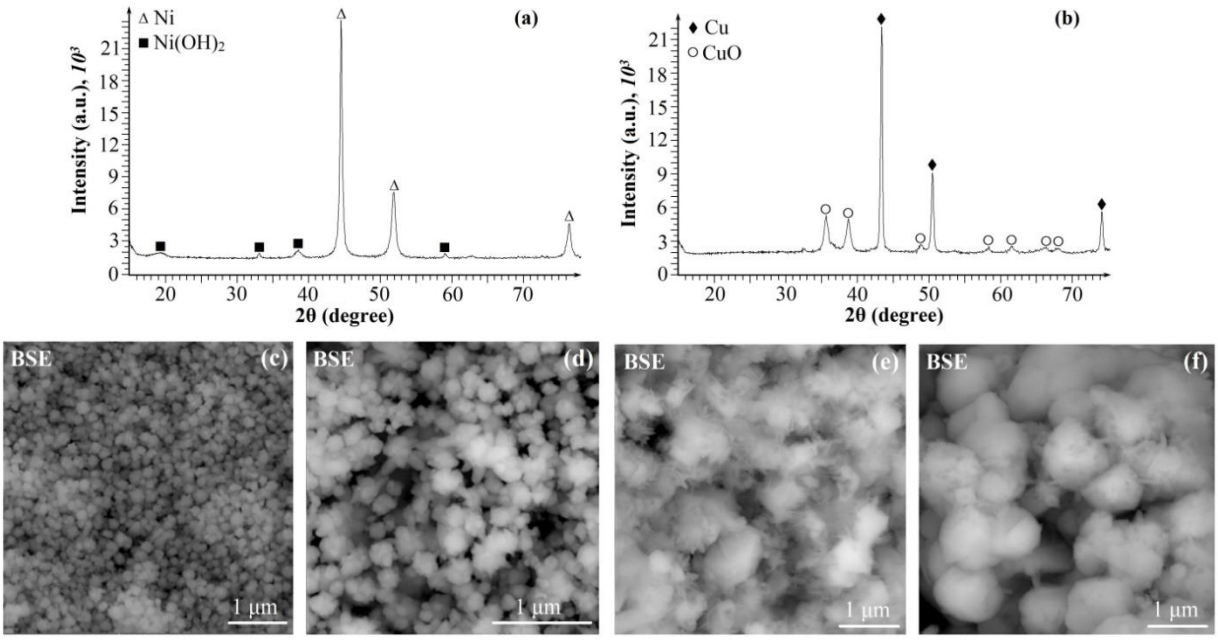

Figure 1. XRD patterns for as-prepared (**a**) Ni and (**b**) Cu nanoparticles; SEM images of (**a, b**) Ni and (**c, d**) Cu particles.

The nickel particle sizes calculated from the Scherrer equation using the diffractometer software are ~26 nm (at an angle 2θ = 44.3°). The reduced copper particles contain a small amount of copper oxide CuO (Figure 1, b). The Cu particles sizes are about 34 nm (at an angle 2θ = 43.2°). When Cu particles are saturated with hydrogen in the electrochemical cell, copper cations are additionally reduced from CuO.

On micrographs (Figure 1, c and d), nickel particles are aggregated in rounded formations with sharp branch pieces. The sizes of these enlarged particles are ~100-180 nm. Copper particles also have a rounded shape, but they are larger than nickel particles, their size is ~0.8 - 1.0 μm (Figure 1, e and

Preprints (www.preprints.org) | NOT PEER-REVIEWED | Posted: 7 July 2023 doi:10.20944/preprints202307.0455.v1

f). They are formed from copper plates of different thicknesses, which can be clearly traced from their micrographs.

In the XRD pattern of bimetallic Ni/Cu-1 particles synthesized by the first synthesis procedure (see in Supplementary part), when the reduced Ni particles are separated from the filtrate, sonicated, and then copper cations are reduced in their presence, there are clear peaks for both metals as well as low peaks for CuO (Figure 2, a). The phase constitution of these particles after their saturation with hydrogen in an electrochemical cell and the use in *p*-NPh electrohydrogenation practically does not change, only the content of copper oxide decreases (Figure 2, b).

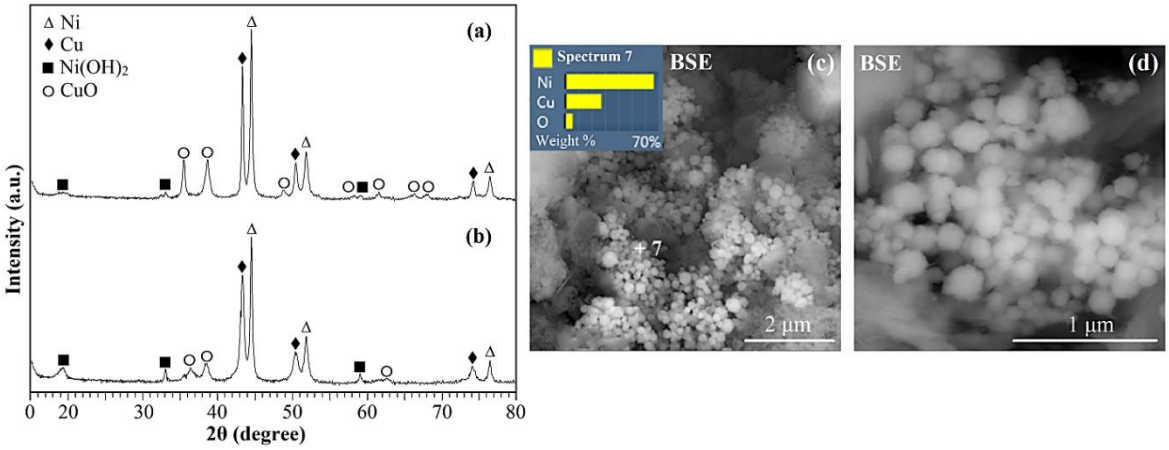

Figure 2. XRD patterns for Ni/Cu-1 particles (**a**) after reparation and (**b**) after electrochemical experiments; (**c, d**) SEM images of bimetallic Ni/Cu-1 particles after preparation.

Micrographs of Ni/Cu-1 particles after their synthesis (Figure 2, c and d) taken with a back scattered electrons (BSE) detector clearly show rounded particles of 60-300 nm in size collected from smaller grains. In the micrographs, these particles are lighter and obviously consist of nickel particles coated with copper. EDS analyzes of these light rounded particles show the presence of both metals with a predominance of one or the other as well as oxygen with a small content (as in the Spectrum of the marked particle). If these are particles consisting of a Ni core and a Cu shell, then their content is determined either by the size of the core or by the width of the shell. It is also noticeable in these micrographs that rounded light particles tend to group into larger agglomerates. In addition, micrographs show that these particles also contain thin plates (~30-70 nm thick) apparently belonging to CuO, which are part of their composition (Figure 2, a).

Successive chemical reduction of Ni^{2+}, then Cu^{2+} cations in the same solution (according to second procedure described in Supplementary part)) is accompanied by the formation of Ni NPs, as can be clearly seen in the XRD pattern of Figure 3, a, but the reduction of Cu^{2+} cations to Cu^0 does not occur. Obviously, the addition of copper salt to an alkaline solution with Ni NPs leads to the appearance of copper hydroxide, $Cu(OH)_2$, from which CuO oxide is then formed. The introduced hydrazine hydrate had no restoring effect. In the electrochemical cell, copper cations are almost completely reduced from CuO as indicated by the diffraction peaks for Cu^0 in the XRD pattern of Ni/Cu-2 particles (Figure 3, b).

Preprints (www.preprints.org) | NOT PEER-REVIEWED | Posted: 7 July 2023 doi:10.20944/preprints202307.0455.v1

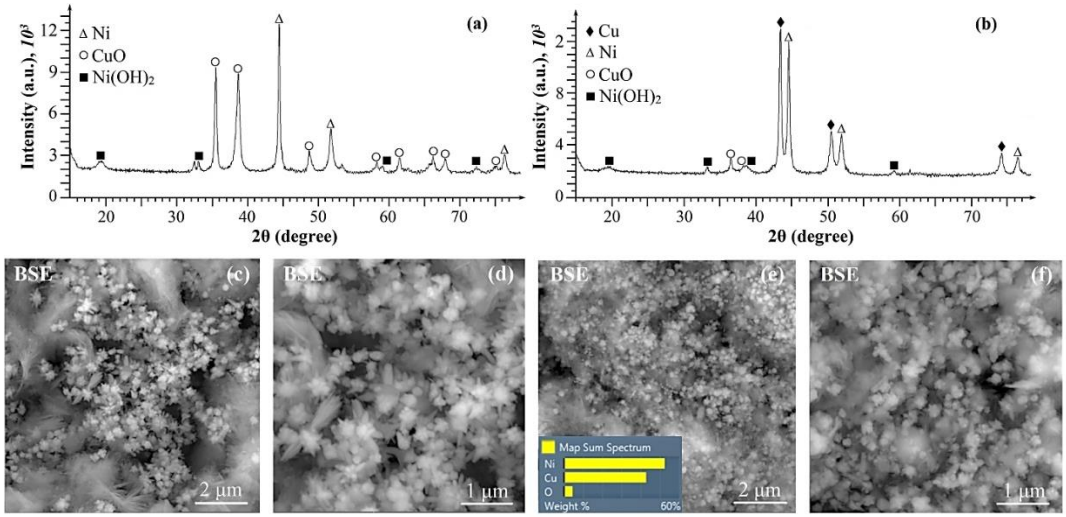

Figure 3. XRD patterns for Ni/Cu-2 particles (**a**) after preparation and (**b**) after electrochemical experiments; SEM images of the particles (**c, d**) after preparation and (**e, f**) after electrochemical experiments.

According to micrographs of Ni/Cu-2 particles after synthesis (Figure 3, c and d), they contain "prickly" nickel particles (~300 nm) and feather-like crystallites of copper oxide (II). After the electrochemical reduction of copper oxide, it would be expected that the nickel particles would be coated with reduced copper shell to form Ni/Cu core-shell particles. In general, EDS mapping of one of the areas of these particles (Figure 3, e) showed the content of metals in them similar to the phase constitution of Ni/Cu-2 particles in their XRD pattern (Figure 3, b). It follows from the micrographs that copper electrochemically reduced from its oxide forms large agglomerates composed of thin copper plates. "Prickly" particles of nickel are preserved, and some of them are covered with a shell of reduced copper (lighter formations in the micrographs of Figure 3, e and f). Nickel "prickles" look out from some particles. EDS analysis showed that these light particles are composed of ~60% nickel, 30-35% copper and oxygen. At the same time, one can also note a tendency to agglomerate both smaller particles and large ones with the formation of various structural forms.

Cu/Ni particles prepared using the two procedures also have some differences in phase constitutions according to XRD analysis (Figure 4, a and b). These differences derive from the intensities of characteristic peaks for copper and nickel metals. Both samples of these particles contain impurities of copper (II) oxide and nickel (II) hydroxide in smaller amounts. As noted above, when Cu/Ni particles are saturated with hydrogen in an electrochemical cell, copper oxide is almost completely reduced with the formation of additional amount of copper, while the content of $Ni(OH)_2$ does not change. Microscopic studies of Cu/Ni particles showed that their compositions contain large agglomerates (up to 3–5 μm in size) from copper plates or flakes, on which "prickly" nickel particles are located (Figure 5, c), as well as nickel particles in the form of pronounced stars distributed among oxide-copper and copper crystallites (Figure 5, d). But even in the structure of Ni stars, EDS analyzes reveal copper (~30-40%) and oxygen (~10%) elements. Obviously, Cu-Ni heterostructural micro- and nanoparticles are formed.

The performance of the synthesis of Ni or Cu particles in the solution with the PVA polymer addition had almost no effect on their sizes. The successive reduction of the second metal in the presence of the obtained first metal particles leads to the formation of bimetallic heterostructural compositions consisting of small "prickly" Ni particles and larger rounded Cu particles, in which the second metal is also found.

Preprints (www.preprints.org) | NOT PEER-REVIEWED | Posted: 7 July 2023 doi:10.20944/preprints202307.0455.v1

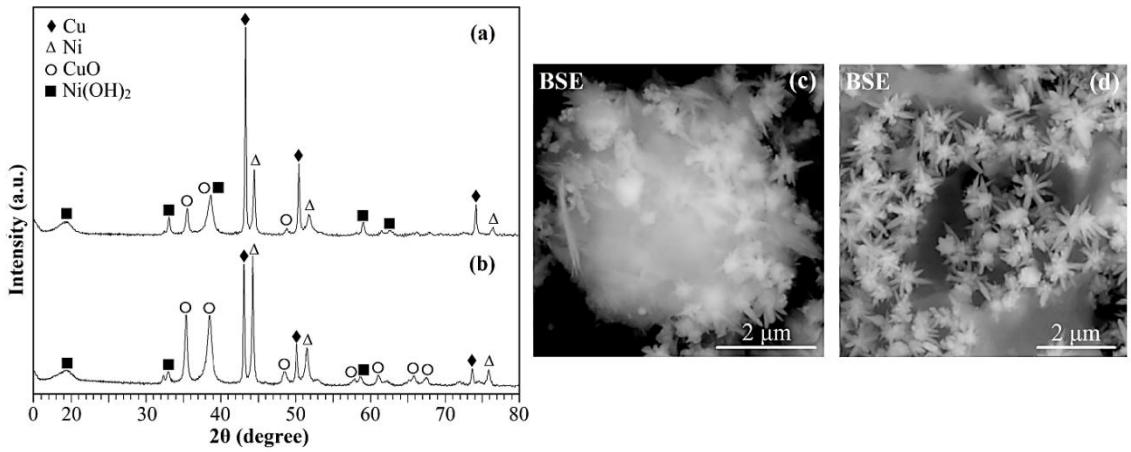

Figure 4. XRD patterns for (**a**) Cu/Ni-1 and (**b**) Cu/Ni-2 particles after preparation and (**c, d**) SEM images of the particles.

The electrocatalytic hydrogenation of *p*-NPh (*p*-NO_2–C_6H_4–OH) over prepared bimetallic Ni/Cu and Cu/Ni micro- and nanoparticle catalysts was carried out in the conditions described in the Experimental part. The results are listed in Table 1. The first columns of this Table contain data on the content of each metal in 1 g of prepared mono- and bimetallic particles. Since their compositions incorporate impurities that were shown by X-ray diffraction analysis, the metal content turned out to be less than 1 g.

Table 1. The results of the *p*-NPh electrocatalytic hydrogenation over the mono- and bimetallic Ni-Cu particles.

Ni, Cu and Ni-Cu particles	Metal content in 1 g of particles, g		Specific surface area, m^2/g	V H_2, mL	Electrocatalytic hydrogenation of *p*-NPh				
					W, mL H_2/min		α, %	Faradaic efficiency, %	
	Ni	Cu			α = 0.25	α = 0.5		α = 0.5	α = 0.75
Cu cathode	-	-	-	-	5.4	4.7	92.3	27.14	17.27
Ni	0.94	-	18.8 ± 0.2	15.7	16.7	16.6	100.0	95.27	86.24
Ni	0.47	-		8.4	12.6	12.0	100.0	69.11	60.09
Cu	-	0.90	6.7 ± 0.1	120.1	17.2	16.7	100.0	96.10	86.24
Cu	-	0.45		58.2	15.8	15.0	100.0	86.02	72.87
Ni/Cu-1	0.46	0.46	11.7 ± 0.1	80.9	17.0	16.8	100.0	96.24	85.64
Ni/Cu + PVA-1	0.48	0.48	15.4 ± 0.1	55.7	15.7	15.3	100.0	88.13	73.31
Ni/Cu-2	0.41	0.41	13.8 ± 0.1	135.7	16.2	15.5	100.0	89.29	73.06
Ni/Cu + PVA-2	0.45	0.45	-	111.2	12.4	11.8	100.0	67.52	59.63
Cu/Ni-1	0.42	0.42	45.5 ± 0.1	59.4	15.5	15.0	99.8	86.15	73.14
Cu/Ni + PVA-1	0.40	0.40	-	34.2	7.0	5.7	100.0	32.74	24.55
Cu/Ni-2	0.42	0.42	30.8 ± 0.4	81.6	14.0	13.2	99.9	80.17	75.86
Cu/Ni + PVA-2	0.49	0.49	-	17.1	12.8	12.2	100.0	70.06	62.16

The synthesized Ni particles are characterized by a larger specific surface area than Cu particles (Table 1), which is confirmed the microscopic studies. The values of the specific surface area of bimetallic Ni/Cu particles are in the range of 11.7-15.4 m^2/g, wherein the initial synthesis of Ni particles using PVA polymer leads to its slight increase. The specific surface area of Cu/Ni particles turned out to be larger, apparently, due to the formation of smaller nickel particles in the shape of stars.

Preprints (www.preprints.org) | NOT PEER-REVIEWED | Posted: 7 July 2023 doi:10.20944/preprints202307.0455.v1

After depositing Ni-Cu particles exhibiting magnetic properties on the cathode surface, they were saturated with hydrogen (stage 1). During this process, hydrogen is absorbed, which is mainly used for the electrochemical reduction of copper cations from its oxide: $CuO + 2e^- + H_2O \rightarrow Cu^0 + 2OH^-$ (in an alkaline solution of catholyte). It was established by verification experiments that nickel cations are not reduced from its oxide and hydroxide under the given experimental conditions, which is obviously due to the negative value of its standard electrode potential (-0.250 V) (for copper it is +0.377 V).

The volumes of hydrogen (V_{H2}) absorbed of mono- and bimetallic particles are shown in Table 1. From their values it follows that almost all bimetallic Ni/Cu and Cu/Ni particles as well as Cu particles absorb hydrogen which indicates the incomplete chemical reduction and instability of copper to oxidation under specified conditions. After the absorption of hydrogen stopped, the organic compound was introduced into the catholyte, and the second stage began – the electrocatalytic hydrogenation of *p*-NPh on Ni-Cu particles additionally reduced upon saturation with hydrogen.

As follows from the data in Table 1, the electrochemical reduction of *p*-NPh on a non-activated cathode in the initial period of the process (α = 0.25) is carried out at a low rate of 5.4 mL H_2/min and incomplete conversion (α = 92.3%). In the UV-Vis spectrum for a diluted catholyte with an initial concentration of *p*-NPh, there is an absorption band for 4-nitrophenolate ion at 403 nm (Figure 5, curve 1). For catholyte after finishing this experiment, the intensity of this band decreases sharply but does not disappear (Figure 5, curve 2), indicating the presence of *p*-NPh, and an absorption band for *p*-APh appears at 314 nm.

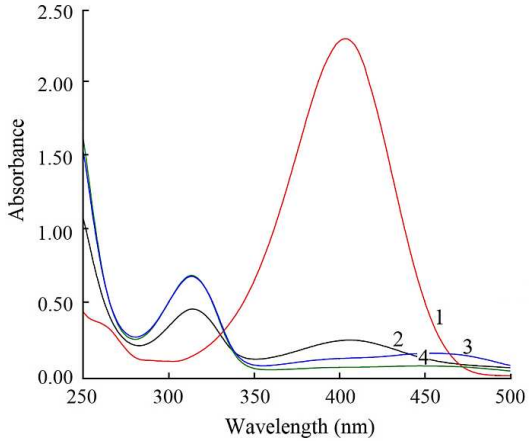

Figure 5. UV-Vis spectra of alkaline solutions of (1) starting catholyte with *p*-NPh and catholytes (2) after its electrochemical reduction and after electrocatalytic hydrogenation on (3) Ni/Cu-2, and (4) Cu/Ni-2 particles.

The electrocatalytic hydrogenation of *p*-NPh on mono- and bimetallic Ni-Cu particles proceeds much more intensively and with the maximum conversion of *p*-NPh than on the pure cathode (Table 1). The best catalytic activity in the *p*-NPh electrohydrogenation was shown by Ni/Cu-1 particles prepared by the 1st procedure and containing particles in core-shell form (Figure 2, c, d). The rate of *p*-NPh hydrogenation using these particles increased more than 3 times compared with the electrochemical reduction of this nitro-compound on the non-activated Cu cathode. The catalytic properties of these particles are evidently determined by the copper shell. In comparison with monometallic copper particles deposited on the cathode in the same amount as contained in Ni/Cu-1 particles (0.45 g), the catalytic activity of these bimetallic particles is higher. All other Ni/Cu and Cu/Ni particles turned out to be less active catalytically and their activity decreases in the following order: Ni/Cu-1 > Ni/Cu-2 > Cu/Ni-1 > Cu/Ni-2. The bimetallic particles obtained using PVA polymer also turned out to be less catalytically active than their corresponding counterparts synthesized without polymer. However, on all tested particles, the degree of *p*-NPh conversion is high with selective formation of *p*-aminophenol. This is confirmed by UV-Vis spectra of catholytes after the

 doi:10.20944/preprints202307.0455.v1

completion of experiments using Ni/Cu-2 and Cu/Ni-2 particles (Figure 5, curves 3 and 4): the *p*-NPh band in the region of 403 nm is practically absent and the *p*-APh characteristic band in the region of 313–314 nm is well identified. The appearance of a low maximum in the region of 460 nm is explained by the property of *p*-APh to rapidly oxidize in light and air with the formation of oxidation products.

For all particle samples used in the electrocatalytic hydrogenation of *p*-NPh, the Faradaic efficiencies for this process were calculated for two values of the degree of conversion of the hydrogenated compound: α = 0.5 and α = 0.75 (Table 1). As follows from the given values, the Faradaic efficiency is quite high in the second half of the process under study and among the bimetallic particles it is the highest for Ni/Cu-1 particles in core-shell form.

3. Experimental Section

3.1. Ni-Cu particles synthesis

The Ni/Cu and Cu/Ni particles were prepared by the successive chemical reduction using two synthetic procedures. Their slight difference lies in the separation of the reduced particles of the first metal from the reaction medium followed by ultrasonic treatment and the addition of a salt of the second metal to the first metal suspension. According to the second procedure, both metals were reduced successive in the same solution. The reducing agent is hydrazine hydrate. The more detailed description of the materials used and synthesis procedures can find in Supplementary part.

3.2. Electrocatalytic experiments

The procedure for electrocatalytic hydrogenation of organic compounds using metal-containing powder catalysts for cathode activation is described in detail in [26, 27]. Experiments on the saturation of powder samples of mono- and bimetallic particles with hydrogen and their subsequent use to activate the Cu cathode in electrocatalytic hydrogenation processes were carried out in a diaphragm electrochemical cell in an aqueous-alkaline solution (the initial NaOH concentration was 2%) at a current of 2.5 A and a temperature of 30°C. A powder of the prepared particles weighing 1 g was deposited on a horizontally located copper cathode (with an area of 0.09 dm^2) tightly adjacent to the bottom of the electrolytic cell. Metal particles with magnetic properties were held on the cathode by an external magnet placed outside the electrolyzer. The magnetic induction of the generated magnetic field is 0.05 T. A platinum grid served as the anode. Electrocatalytic hydrogenation of *p*-NPh (with an initial concentration in the catholyte of 0.04 mol/L) on mono- and bimetallic particles after saturation with hydrogen was also carried out in an aqueous-alkaline solution of the catholyte at a current of 2.5 A, and a temperature of 30°C. The results obtained are presented in Table 1, which lists such characteristics as V_{H2} – the volume of absorbed hydrogen during saturation with it, W – the average rate of *p*-NPh hydrogenation over a period equal to α = 0.25 and 0.5, and α – the *p*-NPh conversion. For the processes of *p*-NPh electrocatalytic hydrogenation, the values of the Faradaic efficiency were also calculated and given in Table 1.

3.3. Physical-Chemical Investigations

The phase constitutions and morphological structure of the synthesized mono- and bimetallic Ni-Cu particles were studied on a Bruker D8 ADVANCE ECO X-ray diffractometer (Bruker, Germany) using CuKα radiation in the angle range (2θ) 15-90°, and a TESCAN MIRA 3 LMU scanning electron microscope (TESCAN, Czech Republic). The energy-dispersive X-ray spectroscopic (EDS) analysis was performed using the X-Act energy dispersion detector.

The specific surface area of some mono- and bimetallic particles were determined by the BET (Brunauer–Emmett–Teller) method using nitrogen adsorption–desorption isotherms on a Sorbi MS instrument (META, Russia).

To confirm the formation of *p*-APh as a product in the processes studied, the UV-Vis spectra of aqueous-alkaline solutions of catholytes before and after electrochemical reduction of *p*-NPh and its electrocatalytic hydrogenation over Ni-Cu particles were measured using a UV-1900i spectrophotometer (SHIMADZU, Japan) in the range of 250-500 nm.

4. Conclusions

Bimetallic Ni/Cu-1 core-shell particles and Ni/Cu-2 and Cu/Ni heterostructural particles with various contents of both metals were synthesized by successive chemical reduction using hydrazine hydrate as reductant. The studies performed have shown that the conditions for the synthesis of these particles carried out in aqueous-ethanol medium have a significant effect on their size, structural forms and electrocatalytic properties. In the electrochemical cell, when copper-containing particles are saturated with hydrogen, copper is additionally reduced from its oxide CuO. Part of the chemically and electrochemically reduced copper forms its large particles, the other part is deposited on the "prickly" nickel particles present in the reaction medium and thus the core-shell and various heterostructural bimetallic formations are formed. All obtained Ni-Cu particles were studied for the exhibition of electrocatalytic activity in the electrohydrogenation of *p*-NPh and almost all the particles showed a relatively high rate of this process and an almost maximum degree of conversion of the hydrogenated compound. Ni-Cu core-shell particles prepared by separating chemically reduced nickel particles from the filtrate and subsequent reduction of copper cations in their presence showed the highest degree of intensification of the studied process increasing the hydrogenation rate by more than 3 times compared to the electrochemical reduction of *p*-NPh on the non-activated cathode. High values of Faradaic efficiency of the process under study were obtained using monometallic Ni and Cu and some bimetallic particles. The main product of electrocatalytic hydrogenation of *p*-NPh over Ni-Cu particles is *p*-aminophenol, which is confirmed by UV-Vis spectra. Prepared Ni-Cu micro- and nanoparticles in various forms have potential applications for electrocatalytic hydrogenation of other nitro-compounds.

Supplementary Materials: The following supporting information can be downloaded at: www.mdpi.com/xxx/s1, Description of the chemical materials used and procedures for the synthesis of Ni-Cu particles by the method of successive chemical reduction.

Author Contributions: Conceptualization, N.M.I.; methodology, N.M.I. and Y.A.V.; investigation, Y.A.S., Y.A.V. and M.E.B.; writing – review & editing, N.M.I. and Y.A.V.; resources, Y.A.S. and Y.A.V.; supervision, Z.M.M.; funding acquisition, Z.M.M.; visualization: Y.A.S. and Y.A.V. All authors have read and agreed to the published version of the manuscript.

Funding: This work was supported by the Science Committee of the Ministry of Science and Higher Education of Kazakhstan Republic (Scientific and Technical Program No. BR10965230).

Data Availability Statement: All relevant data used in this study are presented in the form of figures and tables in published articles, and all data presented in this manuscript are available on request.

Conflicts of Interest: The authors declare that they have no conflict of interest.

References

1. Liu, X.; Wang, D.; Li, Y. Synthesis and catalytic properties of bimetallic nanomaterials with various architectures. *Nano Today* **2012,** 7, 448-466.
2. Gilroy, K.D.: Ruditskiy, A.; Peng, H.-C.; Qin, D.; Xia, Y. Bimetallic Nanocrystals: Syntheses, Properties, and Applications. *Chem. Rev.* **2016**, *116*, 10414-10472.
3. Qiu, J.: Nguyen, Q.N.; Lyu, Z.; Wang, Q.; Xia,Y. Bimetallic Janus Nanocrystals: Syntheses and Applications. *Adv. Mater.* **2022**, *34*, 2102591.
4. Zhai, Y.; Han,,P.; Yun, Q.; Ge, Y.; Zhang, X.; Chen, Y.; Zhang, H. Phase engineering of metal nanocatalysts for electrochemical CO2 reduction. *eScience*. **2022**, *2*, 467-485.
5. Zhang, S.; Zhang, Z.; Zhang, X.; Zhang, J. Novel bimetallic Cu/Ni core-shell NPs and nitrogen doped GQDs composites applied in glucose in vitro detection. *Public Library of Sciences One.* **2019**, 14, e0220005.
6. Yamauchi, T.; Tsukahara, Y.; Sakata, T.; Mori, H.; Yanagida, T.; Kawaic, T.; Wada, Y. Magnetic Cu-Ni (core-shell) nanoparticles in a one-pot reaction under microwave irradiation. *Nanoscale*. **2010**, *2*, 515-523.
7. Senapati, S.; Srivastava, S.K.; Singh, S.B.; Mishra, H.N. Magnetic Ni/Ag core-shell nanostructure from prickly Ni nanowire precursor and its catalytic and antibacterial activity. *J. Mater. Chem*. **2012**, *14*, 6899-6906.
8. Yang, C.; Xue, W.; Yin, H.; Lu, Z.; Wang, A.; Shen, L.; Jiang, Y. Hydrogenation of 3-nitro-4-methoxy-acetylaniline with H2 to 3-amino-4-methoxy-acetylaniline catalyzed by bimetallic copper/nickel nanoparticles. *New J. Chem.* **2017**, *41*, 3358-3366.

9. Hashemizadeh, S.; Biglari, M. Cu:Ni bimetallic nanoparticles: facile synthesis, characterization and its application in photodegradation of organic dyes. *J. Materials Science: Materials in Electronics*. **2018**, *29*, 13025-13031.
10. Fang, Y.; Zeng, X.; Chen, Y.; Ji, M.; Zheng, H.; Xu, W.; Peng, D.-L. Cu@Ni core–shell nanoparticles prepared via an injection approach with enhanced oxidation resistance for the fabrication of conductive films. *Nanotechnology*. **2020**, *31*, 355601.
11. Phinjaroenphan, R.; Boonserm, K.; Rattanasuporn, S. Preparation and Characterization of Bimetallic Cu-Ni and-or Ni-Cu core-shell Nanoparticles. *Naresuan University Journal: Science and Technology.* **2021**, *29*, 54-63. https:// doi.org/10.14456/nujst.2021.16
12. Guo, X.; Xue, F.; Xu, S.; Shen, S.; Liu, M. Coupling Photothermal Effect into Efficient Photocatalytic H-2 Production by Using a Plate-like Cu@Ni Core-shell Co catalyst. *ChemCatChem*. **2020**, *12*, 2745-2751.
13. Hu, H.; Zhang, D.; Yu, W.; Sugawara, K.; Guo, T. Monodisperse and 1D Cross-Linked Multi-branched Cu@Ni Core-Shell Particles Synthesized by Chemical Reduction. *J. Electronic Mater*. **2014**, *43*, 2548-2552.
14. Gong, Z.; Ma, T.; Liang, F. Syntheses of magnetic blackberry-like Ni@Cu@Pd nanoparticles for efficient catalytic reduction of organic pollutants. *J. Alloys Compd*. **2021**, *873*, 159802.
15. Kytsya, A.R.; Bazylyak, L.I.; Zavaliy, I.Y.; Verbovytskyy, Y.V.; Zavalij, P. Synthesis, structure and hydrogenation properties of Ni-Cu bimetallic nanoparticles. *Appl. Nanosci.* **2022**, 12, 1183-1190.
16. Wei, H.; Xue, Q.; Li, A.; Wan, T.; Huang, Y.; Cui, D.; Pan, D.; Dong, B.; Wei, R.; Naik, N.; Guo, Z. Dendritic core-shell copper-nickel alloy@metal oxide for efficient non-enzymatic glucose detection. *Sensors and Actuators B: Chemical*. **2021**, *337*, 129687.
17. Romanovskii, V.I.; Khort, A.A.; Podbolotov, K.B.; Sdobnyakov, N.Y.; Myasnichenko, V.S.; Sokolov, D.N. One-step synthesis of polymetallic nanoparticles in air invironment. *Izv. Vyssh. Uchebn. Zaved. Khim. Khim. Technol.* **2018**, *61*, 42-47. https://doi.org/10.6060/ivkkt.20186109-10.5867a
18. Zhao, P.; Feng, X.; Huang, D.; Yang, D.; Astruc, D. Basic concepts and recent advances in nirophenol reduction by gold and other transition metal nanoparticles. *Coord. Chem. Rev*. **2015**, *287*, 114-136.
19. Zhang, W.; Tan, F.; Wang, W.; Qiu, X.; Qiao, X.; Chen, J. Facile, template-free synthesis of silver nanodendrites with high catalytic activity for the reduction of *p*-nitrophenol. *J. Hazard. Mater.* **2012**, *217-218*, 36-42.
20. Negrete-Vergara, C.; Alvarez-Alcalde, D.; Moya, S.A.; Paredes-Garcia, V.; Fuentes, S.; Venegas-Yazigi, D. Selective hydrogenation of aromatic nitro compounds using unsupported nickel catalysts. *ChemistrySelect.* **2022**, *7*, e202200220.
21. Li, Y.; Cao, Y.; Jia, D. Enhanced catalytic hydrogenation activity of Ni/reduced graphene oxide nanocomposite prepared by a solid-state method. *J. Nanopart. Res.* **2018**, *20*, 8.
22. Ding, J.; Chen, L.; Shao, R.; Wu, J.; Dong, W. Catalytic hydrogenation of *p*-nitrophenol to produce *p*-aminophenol over a nickel catalyst supported on active carbon. *Reac. Kinet. Mech. Cat*. **2012**, *106*, 225-232.
23. Kästner, C.; Thünemann, A.F. Catalytic reduction of 4-nitrophenol using silver nanoparticles with adjustable activity. *Langmuir*. **2016**, *32*, 7383-7391.
24. Din, M.I.; Khalid, R.; Hussain, Z.; Hussain, T.; Mujahid, A.; Najeeb, J.; Izhar, F. Nanocatalytic assemblies for catalytic reduction of nitrophenols: A critical review. *Critical Reviews in Analytical Chemistry*. **2020**, *50*, 322-338.
25. Sun, L.; Deng, Y.; Yang, Y.; Xu, Z.; Xie, K.; Liao, L. Preparation and catalytic activity of magnetic bimetallic nickel/copper nanowires. *RSC Adv*. **2017**, *7*, 17781-17787.
26. Ivanova, N.M.; Soboleva, Y.A.; Visurkhanova, Y.A.; Muldakhmetov, Z. Electrochemical synthesis of Fe–Cu composites based on copper(II) ferrite and their electrocatalytic properties. *Rus. J. Electrochem*. **2020**, *56*, 533-543.
27. Ivanova, N.M.; Muldakhmetov, Z.M.; Soboleva, E.A.; Visurkhanova, Y.A.; Zhivotova, T.S. Metal-carbon composites based on carbonized melamine-formaldehyde polymer and their electrocatalytic properties. *Rus. J. Electrochem*. **2022**, *58*, 946-956.